Key Points:
- Transport model adequately simulates carbonyl sulfide (OCS) mixing ratios during marine influence in a coastal city
- Modeling of OCS needs to improve characterization of transport and boundary layer variability
- The urban biosphere signal is an important contributor to simulated CO_2 mole fractions

Exploring the Potential of Using Carbonyl Sulfide to Track the Urban Biosphere Signal

Gara Villalba[1,2] , **Mary Whelan**[3] , **Stephen A. Montzka**[4] , **Philip J. Cameron-Smith**[5] , **Marc Fischer**[6], **Andrew Zumkehr**[7], **Tim Hilton**[8], **James Stinecipher**[7] , **Ian Baker**[9], **Ray P. Bambha**[10], **Hope A. Michelsen**[11], **Brian W. LaFranchi**[12] , **Carme Estruch**[1] , and **Elliott Campbell**[8]

[1]Institute of Environmental Science and Technology (ICTA), Universitat Autònoma de Barcelona (UAB), Bellaterra, Barcelona, Spain, [2]Department of Chemical, Biological and Environmental Engineering, Universitat Autònoma de Barcelona (UAB), Bellaterra, Barcelona, Spain, [3]Department of Environmental Sciences, Rutgers University, New Brunswick, NJ, USA, [4]NOAA/Global Monitoring Laboratory, Boulder, CO, USA, [5]Lawrence Livermore National Laboratory, Livermore, CA, USA, [6]Environmental Energy Technologies Division, Lawrence Berkeley National Laboratory, Berkeley, CA, USA, [7]University of California, Merced, CA, USA, [8]Environmental Studies Department, University of California, Santa Cruz, CA, USA, [9]Department of Atmospheric Science, Colorado State University, Fort Collins, CO, USA, [10]Sandia National Laboratories, Livermore, CA, USA, [11]Department of Mechanical Engineering, University of Colorado Boulder, Boulder, CO, USA, [12]Aclima, Inc., San Francisco, CA, USA

Abstract Cities are implementing additional urban green as a means to capture CO_2 and become more carbon neutral. However, cities are complex systems where anthropogenic and natural components of the CO_2 budget interact with each other, and the ability to measure the efficacy of such measures is still not properly addressed. There is still a high degree of uncertainty in determining the contribution of the vegetation signal, which furthermore confounds the use of CO_2 mole fraction measurements for inferring anthropogenic emissions of CO_2. Carbonyl sulfide (OCS) is a tracer of photosynthesis which can aid in constraining the biosphere signal. This study explores the potential of using OCS to track the urban biosphere signal. We used the Sulfur Transport and dEposition Model (STEM) to simulate the OCS concentrations and the Carnegie Ames Stanford Approach ecosystem model to simulate global CO_2 fluxes over the Bay Area of San Francisco during March 2015. Two observation towers provided measurements of OCS and CO_2: The Sutro tower in San Francisco (upwind from the area of study providing background observations), and a tower located at Sandia National Laboratories in Livermore (downwind of the highly urbanized San Francisco region). Our results show that the STEM model works better under stable marine influence, and that the boundary layer height and entrainment are driving the diurnal changes in OCS and CO_2 at the downwind Sandia site. However, the STEM model needs to better represent the transport and boundary layer variability, and improved estimates of gross primary productivity for characterizing the urban biosphere signal are needed.

1. Introduction

Cities are home to 50% of the world population and potentially 70% by 2050 (UN/DESA, 2018). Consequently, cities are major energy consumers and contributors of anthropogenic greenhouse gas (GHG) emissions, representing almost two-thirds of the global energy demand and 70% of carbon emissions from the energy sector (IEA, 2016). Aware of their critical role in mitigating GHG emissions, many cities are adopting measures to reduce the impact of energy-intensive activities, such as urban passenger travel, residential heating, and waste and waste-water treatment through initiatives such as the Covenant of Mayors (Covenant of Mayors, 2009) and the Local Governments for Sustainability (ICLEI, http://www.iclei.org). According to the International Energy Agency, cities must take the lead to limit the global temperature increase to no more than 2°C outlined by the Paris Agreement (United Nations/Framework Convention on Climate Change, 2015). To measure the efficiency of reduction strategies and track progress over time to support policy intervention, cities must establish ways of tracking GHG emissions that are consistent, repeatable and reliable.

The most widely used method for GHG emissions accounting at city level is a bottom-up approach based on energy consumption multiplied by emissions factors specific for each type of fuel and process (GPC, 2014;

ICLEI, 2012; Kennedy et al., 2009). There are several standardized methodologies such as those presented by Kennedy et al., but in general most methods involve determining the CO_2 emissions from electricity, heating and industrial fuels, ground transportation fuels, air and marine fuels, industrial processes and waste. Thousands of cities have committed to report their emissions this way by signing the covenant of mayors agreement (Covenant of Mayors, 2009). However, given the vast amount of time and resources required to carry out such bottom-up inventories, generic emissions factors and data assumptions are often used to calculate the carbon footprint potentially resulting in highly inaccurate estimates of GHG emissions. CO_2 emissions estimated this way at the urban scale have been shown to have an uncertainty of 50%–200% (Asefi-Najafabady et al., 2014; J. C. Turnbull et al., 2011). The bottom-up approach also fails to accurately determine the contribution of urban CO_2 capture by green infrastructures, which are currently being promoted as a means to reduce the carbon footprint (Byrne et al., 2020). Some of the limitations include uncertainty in the time scales for respiration (RESP) of carbon previously taken up through photosynthesis and the effect of urban climate and topography on the urban biosphere. Furthermore, equations that predict biomass generation (carbon sequestration) derived from measurements are not applicable to urban green because of its unique form and maintenance (Pataki et al., 2011).

In recent years, "top-down" simulations of GHG at the urban scale have used bottom-up anthropogenic GHG emission inventories to determine urban GHG concentrations using atmospheric and chemical transport models (Feng et al., 2016; J. C Turnbull et al., 2014). In other cases, atmospheric measurements of the CO_2 concentrations are combined with atmospheric chemical transport models to determine the CO_2 emissions through inverse simulations (McKain et al., 2012; Newman et al., 2013; Turner et al. 2016) and flux estimation methods (Mays et al., 2009). These modeling efforts require biogenic emissions as input which are still highly uncertain because there is significant divergence among the various biosphere models that provide this biospheric component of the carbon budget (Pugh et al., 2016; Sitch et al., 2008). The biogenic emissions are further confounded at the urban level because anthropogenic heat fluxes, impervious surfaces, phenological shifts, and air quality can alter spatial and temporal patterns of biogenic carbon fluxes compared to natural systems (Krupa & Manning, 1988; Melaas et al., 2016; Zhao et al., 2016).

Determining the urban biosphere contribution to the urban CO_2 budget from measurements also has its complexity. One approach is to constrain the anthropogenic CO_2 instead by using CO or C^{14}-CO_2 as gas tracers of fossil-derived CO_2 (Campbell et al., 2008; LaFranchi et al., 2013; J. C. Turnbull et al., 2011; J. Turnbull et al., 2009; Levin et al. 2011) (Miller et al., 2012). These studies have served to quantify discrepancies between bottom-up CO_2 inventories with observations, but have not provided much information in terms of the urban biosphere contribution to the overall carbon budget. While anthropogenic tracers exist, biosphere tracers have not yet been applied in urban analysis.

Thus quantifying the contribution of urban vegetation to the overall CO_2 budget in urban areas is a challenge. Several studies have pursued this endeavor, not only to determine the effectiveness of mitigating GHG by incrementing urban green, but also to accurately monitor, report, and verify such strategies. Hardiman et al. (2017) adapts the Vegetation Photosynthesis and Respiration Model (VPRM) to urban phenology for the cities of Massachusetts, and estimates that urban vegetation absorbs 14% of the anthropogenic emissions, but that this benefit is significantly offset by the urban heat island effect and the asynchrony between temporal patterns of biogenic and anthropogenic carbon fluxes (Hardiman et al., 2017). Park et al. also use an optimized VPRM together with Hestia fossil fuel CO_2 emission data and estimate higher biospheric contribution in the Southern California Air Basin, uptaking 20%–24% of the total anthropogenic CO_2 during the daytime (Park et al., 2018). Using a combination of Light Detection and Ranging (LiDAR) and field techniques, another study was able to quantify that the trees of the city of Meran, Italy, were able to sequester only 0.61% of the traffic emissions (Speak et al., 2020). Eddie co-variance flux estimates performed by Velasco et al., however, show that when considering vegetation and soil together, the biogenic component was found to actually add and extra 4.4% to the total CO_2 flux of a neighborhood in Singapore (Velasco et al., 2016).

To further improve understanding of the influence of urban vegetation, here we explore the potential of using the atmospheric tracer carbonyl sulfide (OCS or COS) to provide information about the contribution of the urban biosphere to the overall carbon budget. Observations of OCS concentrations have recently been used to estimate gross carbon uptake of the biosphere at regional and global scales (Campbell et al., 2017;
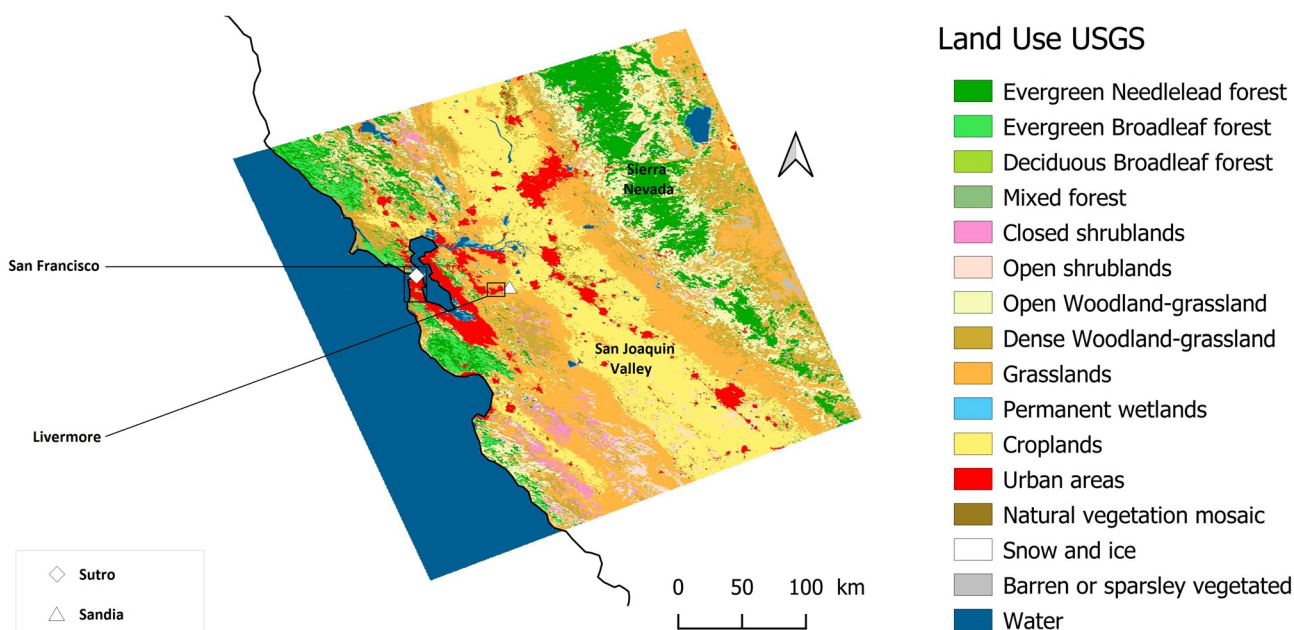
Figure 1. Domain characterization based on United States Geological Survey land categories used for the simulation. The Sandia site is in the city of Livermore, 72 km downwind from the Sutro site located in San Francisco.

Hilton et al., 2017). This technique is based on the close relationship of CO_2 and OCS uptake by plants (Campbell et al., 2008; Sandoval-Soto et al., 2005; Stimler et al., 2011). In contrast to CO_2, plants can take up OCS but do not release it during respiration; this phenomenon allows OCS to be used to estimate the gross primary productivity (GPP) (i.e., the total amount of carbon fixed by photosynthesis in the ecosystem). OCS has been demonstrated to be a good predictor for GPP in forests (Rastogi et al., 2018; Spielmann et al., 2019) and orchards (Yang et al., 2018); although some studies also reported that there is OCS production from marsh vegetation (Whelan et al., 2013), crops (Bloem et al., 2012), and paddy fields (Yi et al., 2008). Previous studies that use OCS as a tracer for GPP have focused on highly vegetated areas at the canopy-scale (Kooijmans et al., 2017) or continental and global scales (Campbell et al., 2017; Hilton et al., 2017).

More recently, high-resolution temporal and spatial surveys of OCS and CO_2 mixing ratios confirm that OCS may be a proxy for CO_2 uptake in homogenous ecosystems on a local scale (Belviso et al., 2016; Campbell et al., 2017). However, less is known about the usefulness of using OCS as a GPP tracer in urban environments, where the complexity of urban and natural activity could include additional sources and sinks of OCS. In this respect, Belviso et al. (2020) conclude that long-range transport of OCS from anthropogenic sources located in Benelux, Eastern France and Germany impacts the Paris area during wintertime, limiting the use of OCS to assess regional-scale CO_2 uptake because of such strong anthropogenic influence. The present study reduces the potential influence of anthropogenic OCS sources by performing the measurements and simulations in the coastal area of San Francisco with frequent westerly winds from the ocean and where the anthropogenic OCS sources have been deemed insignificant (Zumkehr et al., 2018).

On this premise, and with the overall goal of learning how to best quantify the biosphere contribution using OCS as a tracer, we developed a 9-km resolution observation-model framework of the densely populated San Francisco region in California. We used regional atmospheric chemical transport simulations to interpret observed OCS concentrations from an urban tower and explored the drivers of atmospheric OCS variation in the densely populated area.

2. Methods

We use the Sulfur Transport and dEposition Model (STEM) (Carmichael et al., 1991) to simulate the OCS concentrations over the densely populated San Francisco Bay Area at 9-km resolution during March 2015 at one hour temporal resolution. The domain, shown in Figure 1, is a 50 by 50 horizontal grid with 59

pressure-based vertical layers centered around the city of Livermore and is characterized by urban land use, croplands of the San Joaquin Valley, and forests of coastal areas and the Sierra Nevada. There is photosynthetic activity all year in this domain, with the most active period being February through June, which is the wet season. The study captures the month of March, which is the beginning of the most active time of year for photosynthetic activity, peaking in April.

There are two observation towers that provided measurements of OCS and CO_2 for this study. One is the Sutro tower located in San Francisco (37°45′18.72″N, 122°27′10.08″W), which stands 298 m above ground and is 70 km upwind from Livermore. Given its proximity to the ocean and the predominance of westerly winds, Sutro tower provided a representation of background concentrations most of the time. The second tower is located at Sandia National Laboratories in Livermore (Lon: 121.71°, Lat: 37.67) (hereafter referred to as Sandia tower, which is downwind of the highly urbanized San Francisco region with an inlet height of 27 m a.g.l.). OCS and CO_2 samples were collected using 0.7-liter flasks filled to 40 psia over a few minutes at Sutro tower twice a day, which shipped to Boulder, Colorado, for analysis in NOAA's gas chromatography and mass spectrometry laboratory by the methods described by Montzka et al. (2007); at Sandia tower air samples were analyzed hourly, using a Los Gatos Research cavity-enhanced laser absorption spectrometer (Rastogi et al., 2018). CO_2 measurements at Sandia tower were refered to 3 NOAA GMD standards via synthetic air transfer standards. The OCS analyzer was calibrated by a CO_2-referenced method and was thus limited by the uncertainty of the OCS/CO_2 ratio in the standard, estimated to be ±2.8% based on the quadrature sum of the uncertainties in OCS and CO_2 (both ±2%). This included uncertainty in the WMO scale of ±0.07 ppm and repeatability of the transfer of the WMO calibration (based on repeatability during transfer standard calibrations) to the synthetic reference gases of ±0.11 ppm (in total ±0.13 ppm). The median replicate precision for OCS flask samples from the NOAA network was 0.4% (~2 ppt), and 95% of all pairs had a replicate precision of less than 1.3% (<6.3 ppt).

We used the Weather Research and Forecasting model (WRF) version 3.7.1 (Skamarock et al., 2008) using the same domain, vertical profile and time period described above for STEM. The configuration of WRF included the planetary boundary layer (PBL) scheme Mellor-Yamada-Janjic, the Noah land surface model, and the Grell-Devenyi ensemble cumulus scheme (Yver et al., 2013). We ran WRF with reanalysis data provided by the Global Forecast System of NOAA's National Center for Environmental Information at 28-km, 6-hour resolution (NOAA, 2017) to generate the meteorological fields needed to run STEM for March 5–25, 2015 (discarding the first 5 days of the run as spin-up period). The hourly WRF output was validated for surface temperature at 2 m and wind speed and direction at 10 meters observed at the Lawrence Livermore National Laboratory weather station, and provided by https://weather.llnl.gov (see Supporting Information S1).

In addition to the meteorological data, we generated hourly surface fluxes of OCS and CO_2 as input to STEM for the same time period March 5–25, 2015. We used a global OCS hourly inventory of the biospheric surface-flux at 1.25° × 1° resolution (approximately 87 km by 87 km for this latitude) that was produced by the Simple Biosphere Model SIB3 (Baker et al., 2009; Berry et al., 2013). This inventory was regridded to 1-km resolution using normalized difference vegetation index (NDVI) as a spatial proxy for the STEM regional domain (NASA and USGS, 2017). The steps were to first download modis terra NDVI values in text format at the desired resolution from http://modis-land.gsfc.nasa.gov/vi.html. Next, we ran a fortran script to match the NDVI values tot eh STEM domain based on the longitude and latitude of each pixel. The result was a map of NDVI values for each cell (1 km by 1 km) of the entire STEM domain. Then we used the OCS flux data from SiB and the following simple equation to determine the OCS value for each cell (or each pixel) of the STEM domain:

$$\frac{\text{NDVI value of 1 STEM pixel}}{\text{NDVI value of entire STEM domain}} \times \text{OCS flux value of entire STEM domain} = \text{OCS value of 1 STEM pixel}$$

According to this method, the hourly average OCS flux field generated for the entire study period is presented in Figure 2 at 1 km resolution. The supporting information summarizes the input required for running STEM in Figure S3.

Global CO_2 fluxes for GPP and RESP are available from the Carnegie-Ames-Stanford-Approach (CASA) ecosystem model at 1° by 1.25° resolution (NACP, 2015). We regridded each flux from its native grid and resolution to the 50 × 50 grid at 9 km resolution used in this study using the mass-conservative algorithm of the
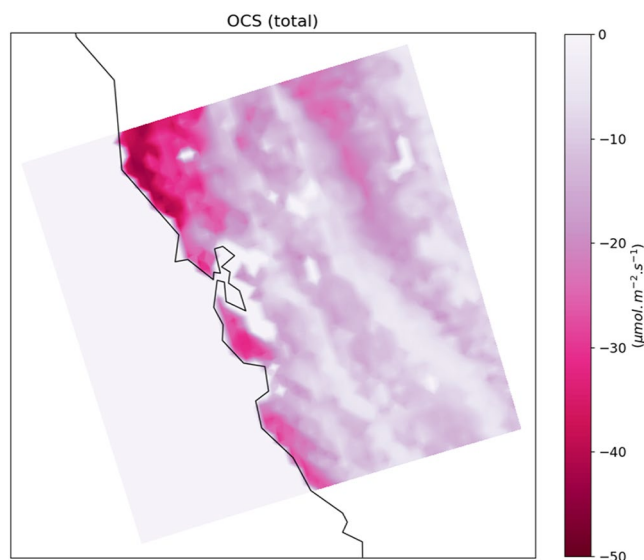
Figure 2. Carbonyl sulfide (OCS) average plant fluxes apportioned using normalized difference vegetation index (NDVI) over the study area. The flux is negative because plants take OCS out of the atmosphere where it becomes destroyed by irreversible hydrolysis. NDVI extracted from MODIS/Terra Vegetation Indices provided by NASA and United States Geological Survey.

MTXCPLE program of the Models-3/EDSS Input/Output Applications Programming Interface (Coates, 2014). Figure 3a (GPP) and Figure 3b (Respiration) show the regridded fluxes. We used the U.S. high resolution inventory for the fossil-fuel derived anthropogenic CO_2 emissions (Gurney et al., 2009; NACP, 2010). This emissions inventory is available hourly at a 10-km resolution, and was regridded to the 9-km resolution as well (see Figure 3c). Unlike the other emissions inventories that were available for the study period, the Vulcan inventory was only available for 2008. Net ecosystem exchange (NEE) is the net exchange of C between the ecosystem and the atmosphere (Kramer et al., 2002). Here we define NEE as the CO_2 released to the atmosphere by RESP minus the CO_2 sequestered by GPP; a sum of all these fluxes results in total CO_2 anomaly from the background (total CO_2 anomaly = ANTHRO CO_2 + NEE) (Figure 3d).

3. Results and Discussion

3.1. Background Climatology

Figure 4 shows long term observation from the NOAA measurements of flasks collected on the Sutro tower, which is usually upwind from the study area of Livermore and provides background mixing ratios for both OCS and CO_2. Comparisons to results from other surface sites in the NOAA network (Montzka et al., 2007, and updates available at ftp://aftp.cmdl.noaa.gov/hats/carbonyl_sulfide/) suggest that the data from Sutro are typically representative of the OCS mole fractions in background air: (a) The mean mixing ratio measured between 2007 and 2015 of 493 ppt is very similar to the mean measured for Niwot Ridge, Colorado, (494 ppt), which is relatively close in latitude in the Northern Hemisphere (40°N, 106°W); (b) the mean Sutro value is only slightly higher than the mean value of 475 ppt at Trinidad Head (California), which is a coastal site north of Sutro and close to the boarder to Oregon (41°N, 124°W), which is consistent with the observation that OCS mole fractions decrease with higher latitudes in the Northern Hemisphere; (c) the OCS mixing ratios at Sutro do not have strong long term trends, which is also suggested for air at more remote, background sites in the NOAA record; and (d) the seasonality of OCS (phase and amplitude) at Sutro is similar in magnitude to other Northern Hemisphere sites in the NOAA network. The observed average OCS concentration during the study period of March 5–25, 2015 is 505 ppt. This value is used as the background value to initialize the OCS in the STEM model runs. A constant initial condition of OCS seems adequate for this study because our interest is in determining the enhancements rather than absolute concentrations. Furthermore, STEM simulations of OCS fluxes in North America run under different initial conditions showed that GPP variability dominates STEM boundary conditions for OCS concentrations (Hilton et al, 2017).

Sutro tower CO_2 observations also show the seasonal variation established by other studies with higher values of CO_2 in winter and lower values in summer (Sweeney et al., 2015). The enhanced mole fraction in the winter indicates an urban influence, mainly attributed to the urban biospheric component acting as a source in winter, rather than a sink as it does in the summer (Miller et al., 2012). The average CO_2 concentration during the study period of March 5–25 is 405 ppm, similar to background concentrations reported by other monitoring stations such as Mauna Loa, Hawaii, United States (NOAA, 2015). We use this value of 405 ppm as background for the CO_2 model runs.

3.2. Urban Observations

We compared background observations at Sutro tower with downwind concentrations at Sandia Tower in Livermore. Background CO_2 measured at Sutro are relatively stable, while at Sandia, CO_2 concentrations follow a strong diurnal cycle. The result is consistent with the expectation that Sutro air typically represents a relatively stable clean marine boundary layer without recent anthropogenic input, whereas the Sandia
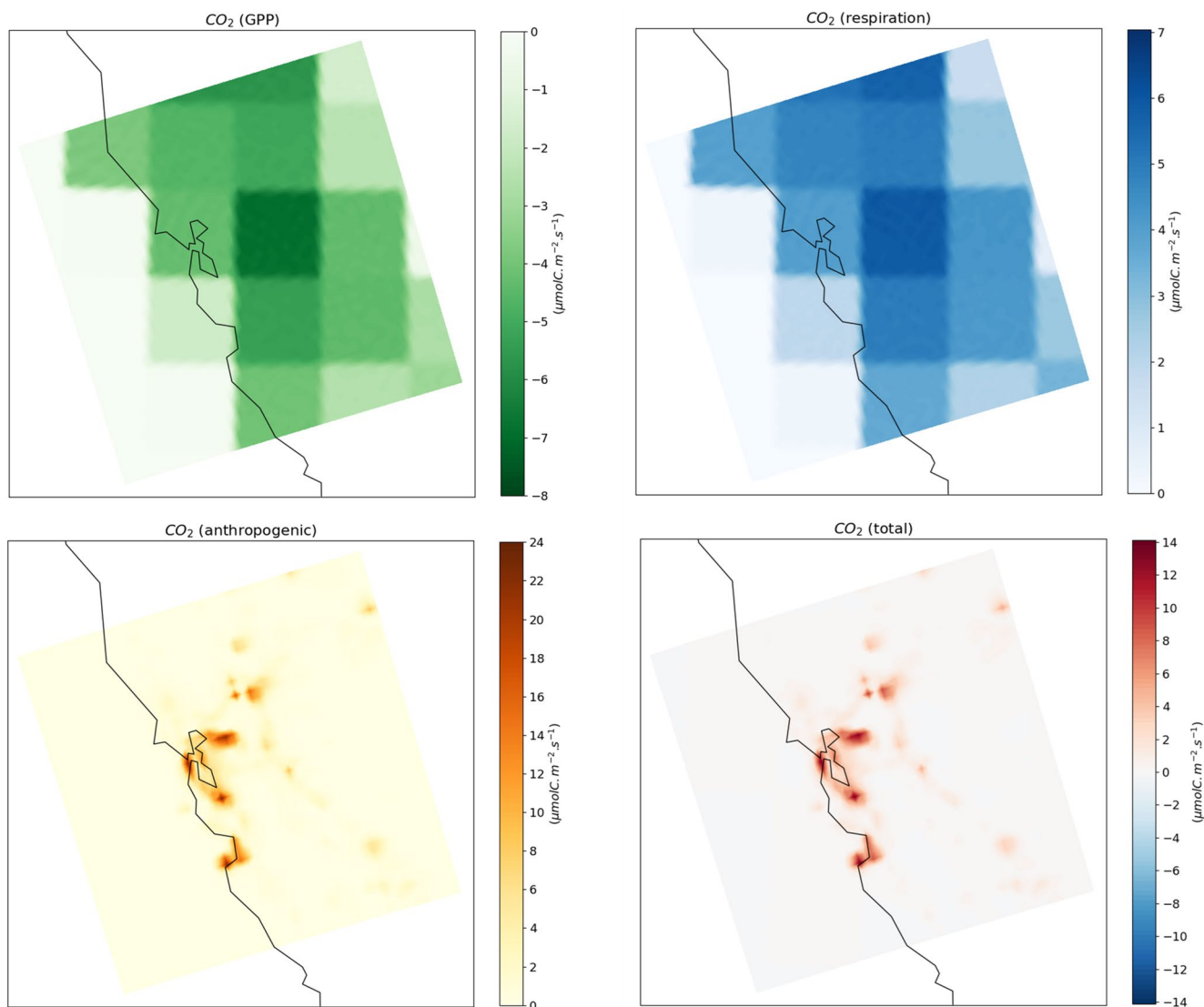
Figure 3. Average hourly fluxes regridded at 9 × 9 km for the study area and simulation period: (a) Gross primary productivity fluxes (Carnegie-Ames-Stanford-Approach (CASA)), (b) Respiration fluxes (CASA), (c) anthropogenic fluxes (Vulcan), and (d) total CO_2.

samples were taken in a continental boundary layer (BL) downwind of an urban region and from a continental boundary layer with high diurnal variability in thickness.

CO_2 mixing ratios are higher at Sandia than Sutro, reflecting the larger impact of anthropogenic sources within the San Francisco region on air downwind of this urban region. The CO_2 observations at Sandia follow a clear diurnal pattern. Concentrations are higher at night and early morning, which is typical of urban areas that are characterized by dominant anthropogenic sources and a diurnally varying boundary layer that is shallowest at night time. The lowest CO_2 concentrations at the Sandia tower location occur at noon, when vertical mixing is enhanced at photosynthetic rates are elevated. Highest CO_2 enhancements relative to background occur at nighttime when plant CO_2 assimilation, anthropogenic activity, and PBL height are all at a minimum. The enhancement maxes despite anthropogenic emissions being at a minimum because the low PBL height and no C uptake by plants is more than enough to compensate for the drop in anthropogenic emissions. Similarly, a study performed for the city of Salt Lake City by McKain et al. (2012) found that the highest concentrations of CO_2 occurred during nighttime and early morning (up to 60 ppm above background values), notably out of phase with anthropogenic emissions, which are elevated during the day. The study by McKain also found that CO_2 concentrations were lowest from 12 to 8 p.m, with enhancements
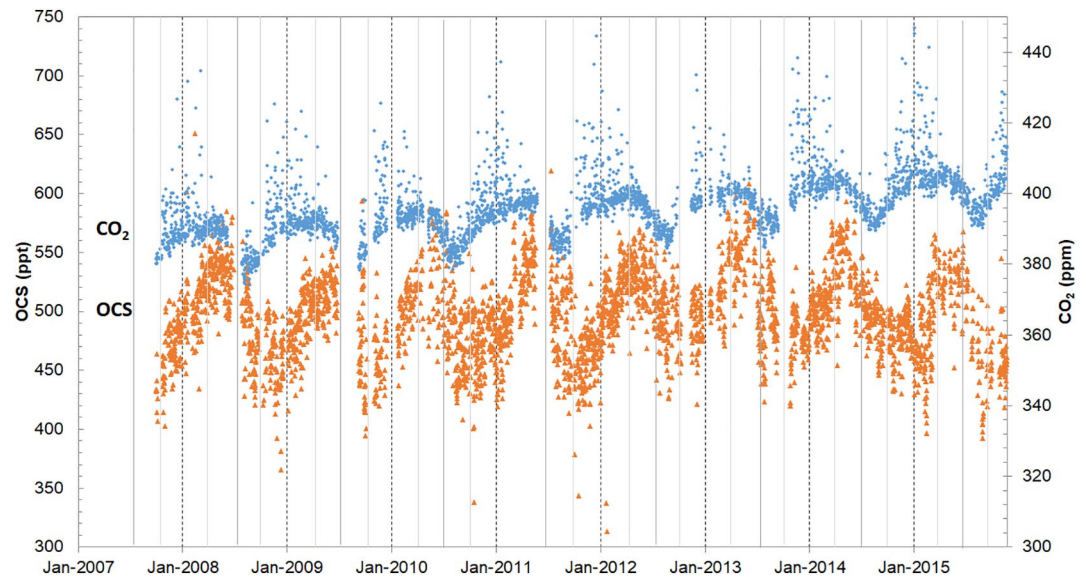
Figure 4. Observations from flasks collected at Sutro tower for atmospheric mole fractions of carbonyl sulfide and CO_2 from October 2007 to December 2015.

relative to background of 0–20 ppm. In natural ecosystems, where there are no other sources of CO_2 other than soil and day-to-night differences in CO_2 are attributed to GPP and RESP (Knox et al., 2018). This explanation may not apply to urban areas, where anthropogenic CO_2 emissions are expected to dominate local mole fractions. In an attempt to separate anthropogenic from biogenic sources of urban CO_2, Wei et al. (2020) attributed the highest CO_2 at early morning (7:00) to the unusual high traffic during this time, with a peak-to-peak amplitude of 12.5 ppm compared to lower values occurring at midday (14:00), when atmospheric boundary-layer mixing and biogenic uptake (i.e., photosynthetic peak) maximize reducing atmospheric CO_2 mole fractions.

The lower panel of Figure 5 shows the observed concentrations of OCS. At Sutro, OCS mixing ratios showed variability between 450 and 550 ppt until March 21, at which point the concentrations stabilized around 550 ppt. One potential explanation for this change in OCS concentration is that continental air can sometimes be transported offshore in the residual layer and then entrained in the marine boundary layer, as was found by Riley (2005). This hypothesis is further validated by the fact that, after March 21, there were stable westerly winds that transported constant OCS (background) concentrations from above the ocean. Before March 21, the wind vectors indicate that the air was from the continent and thus OCS mole fractions may vary according to the degree to which the different air masses were exposed to biosphere OCS sinks over land (see animation available at https://ddd.uab.cat/record/232963). Another potential explanation could be that changes in the boundary layer depth could cause Sutro tower to sometimes sample in the continental boundary layer and some other times in the free troposphere.

The mixing ratios of OCS at the Sandia location were on average 40 ppt lower than at the Sutro tower location, which may reflect the strong OCS plant sink (Campbell et al. 2008) existing between the two towers. Typically OCS concentrations peaked at midday/early afternoon and were lowest at midnight. This variability is similar with other studies of the continental boundary layer (Berkelhammer et al., 2014), which show that OCS mixing ratios are highest in the middle of the day because of deep boundary layer depths, causing increased mixing with the free troposphere, which has a greater effect on the diurnal variation in the mixing ratio than the capture of OCS by photosynthesis. This mixing effect in the middle of the day is also true for CO_2, as can be seen by the lower mixing ratios at noon in Figure 5a.
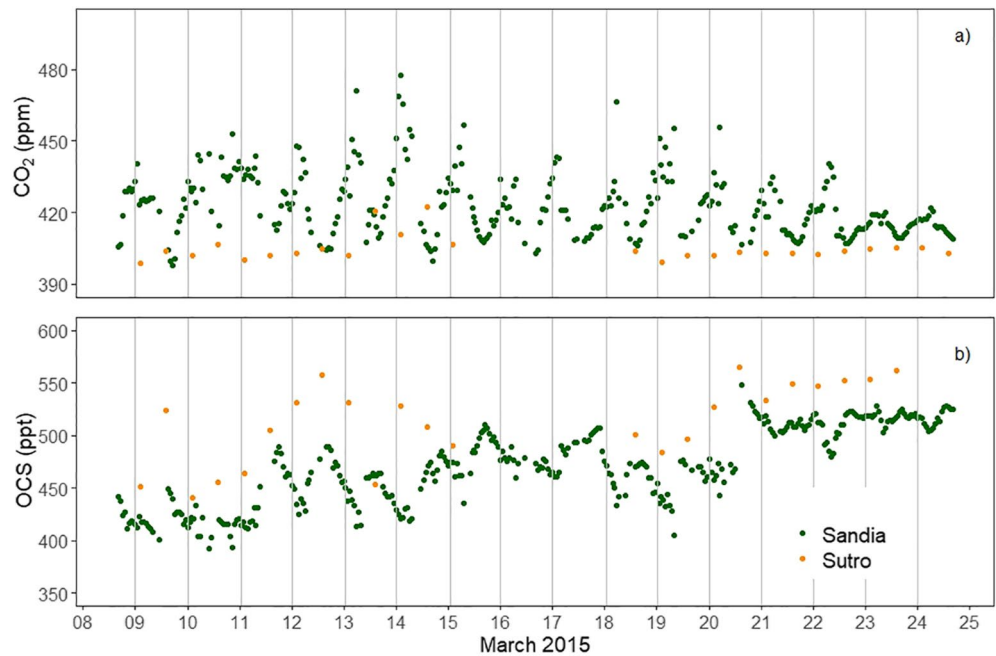
Figure 5. Observed mixing ratios of CO_2 (above) and carbonyl sulfide (below) at the two towers of observation: Sutro tower (background, predominantly marine influence), and Sandia tower (continental influence). The vertical lines represent midnight local time PST.

3.3. Simulated OCS

Simulated OCS concentrations were compared to observed concentrations at the Sandia location, as shown in Figure 6. After March 20, both the observed and simulated mixing ratios exhibited lower day-to-day variability than the earlier period. The earlier part of the period had a synoptic system causing irregular flow, but after March 20 wind patterns returned to a typical summer regime for this region of northwesterly flow. The observations reflect this better than the simulations, which are much more consistent due to the fixed lateral boundary conditions used in the simulations, limiting the capability of our model for interpreting
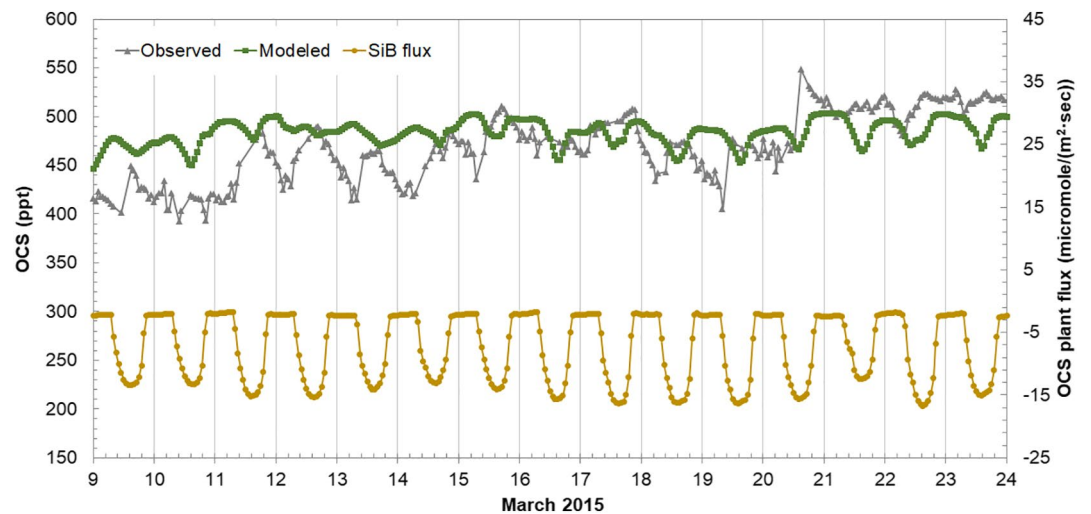

Figure 6. Carbonyl sulfide (OCS) mixing ratios from observations (gray) and model simulations (green) at the Sandia are shown on the left-hand vertical axis, whereas the input flux of OCS (micromole/m²/sec) from the Simple biosphere model (SIB3 flux) is given on the right-hand vertical axis. The vertical lines represent midnight local time PST.
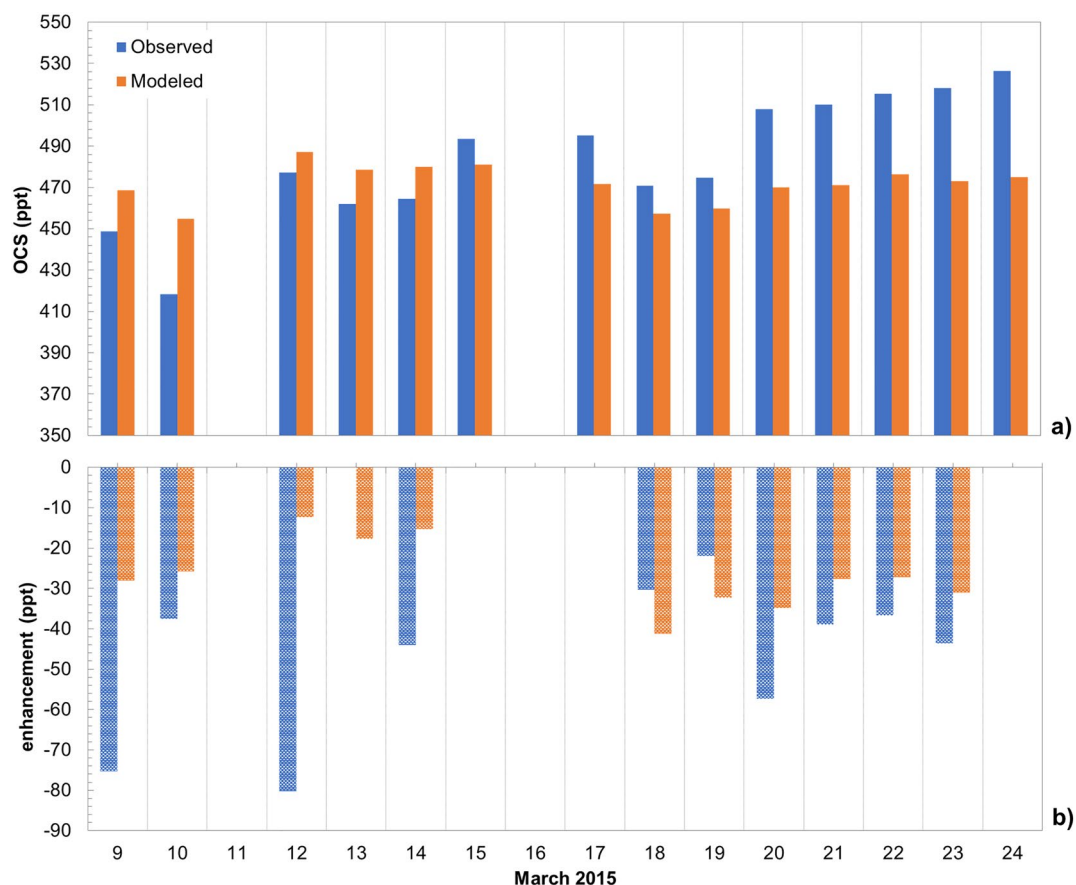
Figure 7. (a) 3-Hour average mixing ratios of carbonyl sulfide observed (blue) and modeled (red) at the Sandia location. The averages are calculated between 12:00 and 15:00 for March 9th-March 24th at local time PST; (b) the observed mole fraction enhancement (blue) is calculated as the difference between the mixing ratios observed at the Sandia tower and Sutro tower at 14:00 local time PST. The modeled enhancement (red) calculated as the difference between the mixing ratios of the two towers averaged over a three-hour period in the afternoon (12:00, 13:00, 14:00, and 15:00), local time PST.

this trend. An animation of OCS fluxes (micromole/m^2/s) and drawdown (ppt) is available at https://ddd. uab.cat/record/232963.

Figure 6 shows that the simulation result includes a significant bias at night, which may be due to typical deficiencies in modeling the PBL depth during this time. This bias is most apparent prior to March 21, at which point there was a shift from continental to marine air (please refer to Figure S4 in the supporting information for a graphical representation of the bias). After March 20, observed mixing ratios were higher, and the modeled mixing ratios enter a more standard diurnal pattern (hitting 500 ppt every night and dropping around noon every day). This latter pattern is due to the fact that after March 20 there are strong westerly winds and a consistent marine influence, as opposed to the continental influence occurring before March 20, which resulted in less stable patterns. Figure 6 also shows that the model underpredicts measured OCS mole fractions after March 20 indicating an overestimation of OCS uptake by urban vegetation by the STEM model or underestimated OCS fluxes from the SiB model. Wind direction is decisive in the interpretation of OCS values in regions with heterogeneously dispersed sources and sinks; in a recent study, (Belviso et al., 2016) described nighttime transport of anthropogenic sources of OCS related to changes in winds directions.

Modeled and observed average daily OCS mixing ratios at the Sandia location for the times 12:00 to 15:00 are shown in Figure 7a. We concentrate the study on this period because it is when the biosphere sink is expected to be the most significant. Additionally, the PBL height as simulated by WRF is lower than the height
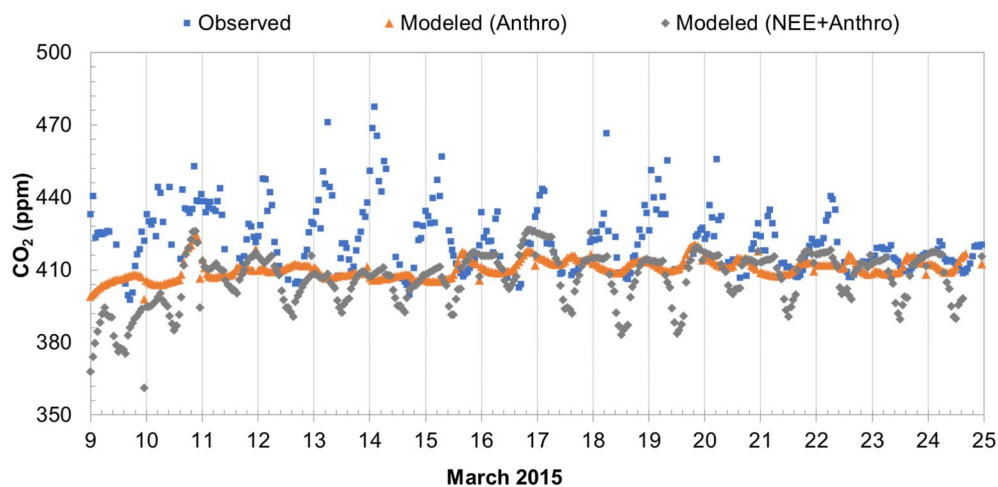
Figure 8. Modeled and observed CO_2 mixing ratios at Sandia. The vertical lines represent midnight local time PST.

derived from radiosonde measurements from NOAA/ESRL Radiosonde Database for Oakland (NOAA/ESRL, 2015) area and the Heffter (1980) method during evening and early hours, while more agreement was found at midday-a known limitation in WRF simulations (Jia & Zhang, 2020). (See Supporting Information S2 for PBL simulations, calculations, and method description). The big discrepancy between modeled and observed OCS values at maximum photosynthetic rates suggest that the model is not well suited for determining GPP. The agreement between the modeled and observed enhancements improves considerably toward the end of the study period after the synoptic system has passed, as shown in Figure 7b, where the enhancement of OCS concentrations is calculated as the difference between the concentrations at Sandia minus the concentration at Sutro for the same hour period.

3.4. Simulated CO_2

Figure 8 compares modeled (initialized with Sutro tower data) and observed CO_2 at the Sandia tower location. The modeled CO_2 includes NEE and anthropogenic emissions of CO_2. During the continental influence on air sampled at Sandia during the earlier period, there is a large bias between 10 p.m. and 7 a.m., in which observed CO_2 mole fractions were higher than modeled CO_2, ranging from 20 to 72 pm. The model does a better job during midday (11 a.m.–3 p.m.), when the bias is reduced to 0–15 ppm. During the more typical marine influence after March 20th, the bias is improved overall, but the model performs worst at midday (11 a.m.–3 p.m., bias ranges from 15 to 45 ppm). There are several potential reasons for this discrepancy. One possible answer is that the biosphere uptake signal is being overestimated by the model; in fact we can observe during the whole period that modeled CO_2 is lower in the model than in the observed values. The anthropogenic signal (represented by orange triangles in Figure 8) seems to be underestimated by the model, and it is more notable during nighttime when CO_2 values are much greater than observed values at midday. This explanation is difficult to confirm because there could be model deficiencies in simulating the boundary layer depth that could also be affecting modeled mixing ratios (Hu et al., 2010). In Figure 9, we plot concentrations of CO_2 only for the time period 12–3 p.m., which has been documented as being the time period with best model performance in terms of boundary layer height; this result is consistent with other studies that show a better performance during daytime for modeling boundary layer and wind (Lee et al., 2011).

Figure 9 shows 3-hour averages (between 12 and 3 p.m.) of CO_2 mole fractions from simulations that include different CO_2 fluxes (NEE CO_2 and anthropogenic CO_2 from Vulcan), and they are compared to observed CO_2 concentrations. A comparison of modeled values in Figure 9 show that the biosphere signal is an important contributor to simulated CO_2 mole fractions. This apparent influence could be attributed to two hypotheses: (a) That the biotic signal is overestimated in the model resulting in higher capture of CO2 than observed and/or (b) the anthropogenic flux used as input to the model is perhaps underestimated, also resulting lower values of CO_2 than the observed. Normally, the difference between modeled NEE CO_2 and
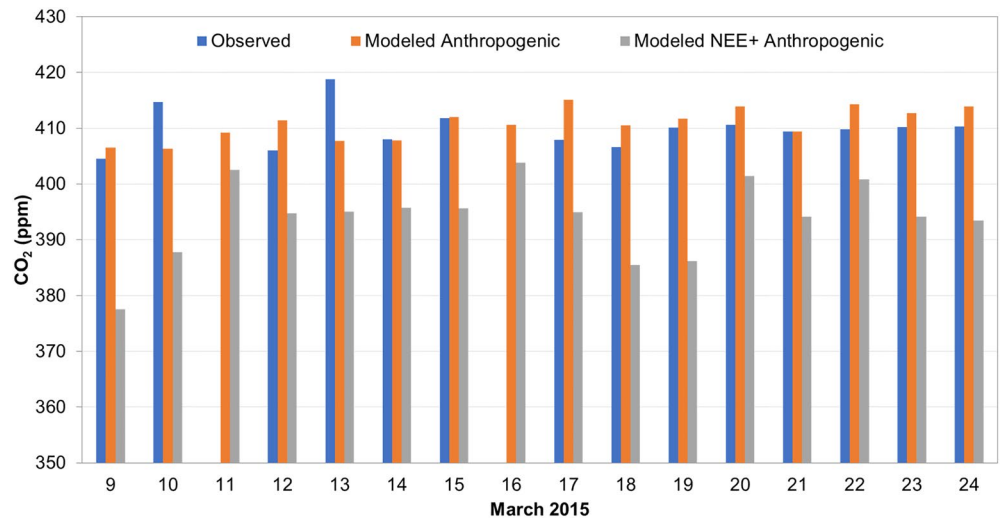
Figure 9. 3-hour averages (between 12:00 and 15:00) of observed, anthropogenic (modeled Vulcan emissions), and modeled total (net ecosystem exchange plus anthropogenic) CO_2 concentrations.

observed CO_2 is attributed to anthropogenic CO_2 (McKain et al., 2012; Wei et al., 2020). However, Figure 9 shows that there is a significant difference between the modeled anthropogenic CO_2 concentrations (orange bars) and the sum of NEE and anthropogenic CO_2 concentrations (gray bars). This difference, which ranges between 9 and 29 ppm, is in the same order of magnitude as the overall model bias. On average, the model bias is 35 ppm. The average contribution from the biosphere is 17 ppm. These results show that the contribution of the urban biosphere is significant, and it is important to quantify it with a certain degree of confidence. The use of OCS as biosphere tracer should improve our estimations of NEE by improving our capacity to fine-tune the GPP signal.

Modeled mixing ratios of OCS and CO_2 present the same problem: They both have bias at night due to deficiencies in modeling the PBL. OCS is biased in the opposite direction to CO_2 because OCS is a small sink at night (Belviso et al., 2020; Maseyk et al., 2014), while CO_2 is a source at night due to respiration. Figure 10 shows the correlation between OCS model error and CO_2 model mismatch. This correlation is a strong indicator that model mismatch is due to transport, not due to model input of sinks and sources.
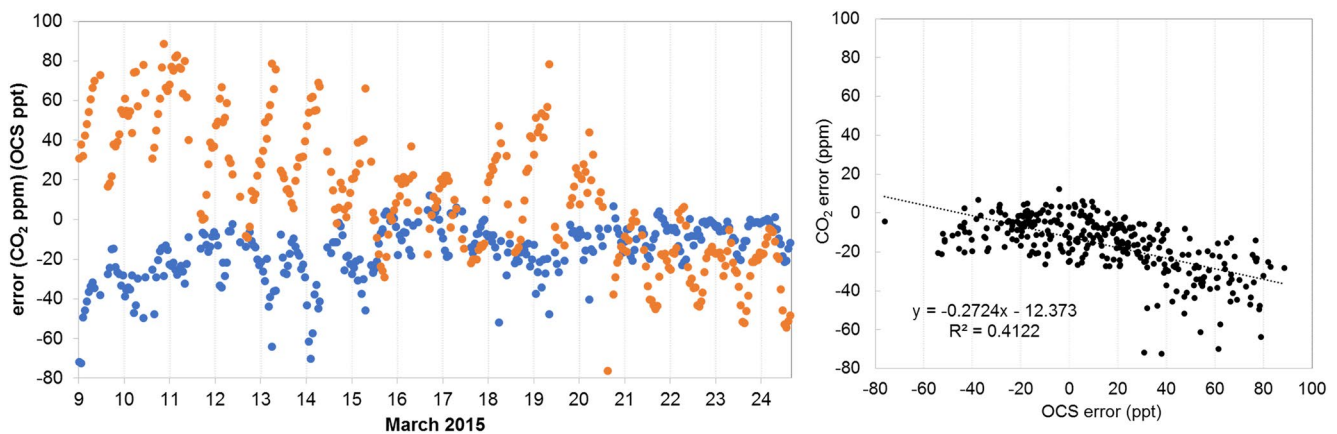

Figure 10. Model mismatch between CO_2 and carbonyl sulfide from Sulfur Transport and dEposition Model. The vertical lines represent midnight local time PST.

4. Conclusions

This study evaluates and describes the present limitations of using OCS as a tracer of the urban biosphere to determine the contribution of the urban ecosystem to CO_2 uptake. We used the STEM to simulate the OCS concentrations and the CASA ecosystem model to simulate global CO_2 fluxes over the Bay Area of San Francisco during March 2015. Our results show that the STEM model works better under stable marine influence, and that theBL height and entrainment are driving the diurnal changes in CO_2 at the downwind Sandia site. However, the model needs a better characterization of transport and BL variability and improvements in the estimation of GPP for characterizing the urban biosphere signal. A synoptic event in the middle of our run clearly shows a shift in the background concentrations, evidencing a shift from continental to marine influence. The transport model does a better job simulating OCS concentrations during the marine influence, when Sutro tower can be assumed to be representative of background concentrations. BL depth is more important in driving diurnal variability in mixing ratios than CO_2 emissions in the urban area. This conclusion is supported by the fact that we found more CO_2 emissions but lower mixing ratios in the afternoon than in the evening, due to the reduction in the the BL depth at night.

The chemical transport model STEM is not correctly representing the diurnal cycle we see with observations reflecting deficiencies in its transport feature (how wind and boundary layer depth affect fluxes) or in the quantification of fluxes affecting CO_2 and COS. Furthermore, we identify the need to improve the model in terms of daytime mixing ratios of biogenic emissions to be able to refine GPP predictions. However, we also show that the "enhancement" of urban OCS concentrations (compared to the background) agrees with modeled enhancement when the observed background OCS values are stable during the period of marine influence.

Data Availability Statement

The data on which this article is based are publically available at the following web sites: The reanalysis meteorological data used for the WRF runs are available in https://www.ncdc.noaa.gov/data-access/model-data/model-datasets/climate-forecast-system-version2-cfsv2; temperature at 2 m and wind speed and direction at 10 meters from the Lawrence Livermore National Laboratory weather statio are available at https://weather.llnl.gov; hourly OCS flux data for the STEM runs were extracted from the OCS hourly inventory of the biospheric surface-flux at 1.25° × 1° resolution (Baker et al., 2009; Berry et al., 2013); NDVI data used in this study was downloaded from http://modis-land.gsfc.nasa.gov/vi.html; Global CO_2 fluxes for GPP and RESP are available at https://nacp-files.nacarbon.org/nacp-kawa-01/; U.S. high resolution inventory for the fossil-fuel derived anthropogenic CO_2 emissions were downloaded from the Vulcan inventory https://daac.ornl.gov/NACP/guides/Vulcan_V3_Annual_Emissions.html; Radiosonde measurements were obtained from https://ruc.noaa.gov/raobs/.

References

Asefi-Najafabady, S., Rayner, P. J., Gurney, K. R., McRobert, A., Song, Y., Coltin, K., et al. (2014). A multiyear, global gridded fossil fuel CO_2 emission data product: Evaluation and analysis of results. *Journal of Geophysical Research: Atmosphere*, *119*(17), 10210–10231. https://doi.org/10.1002/2013JD021296

Baker, I. T., Prihodko, L., Denning, A. S., Goulden, M., Miller, S., & Da Rocha, H. R. (2009). Seasonal drought stress in the amazon: Reconciling models and observations. *Journal of Geophysical Research*, *114*(1), G00B01. https://doi.org/10.1029/2007JG000644

Belviso, S., Lebegue, B., Ramonet, M., Kazan, V., Pison, I., Berchet, A., et al. (2020). A top-down approach of sources and non-photosynthetic sinks of carbonyl sulfide from atmospheric measurements over multiple years in the Paris region (France). *PLoS One*, *15*(2), e0228419. https://doi.org/10.1371/journal.pone.0228419

Belviso, S., Reiter, I. M., Loubet, B., Gros, V., Lathière, J., Montagne, D., et al. (2016). A top-down approach of surface carbonyl sulfide exchange by a Mediterranean oak forest ecosystem in southern France. *Atmospheric Chemistry and Physics*, *16*(23), 14909–14923. https://doi.org/10.5194/acp-16-14909-2016

Berkelhammer, M., Asaf, D., Still, C., Montzka, S., Noone, D., Gupta, M., et al. (2014). Constraining surface carbon fluxes using in situ measurements of carbonyl sulfide and carbon dioxide. *Global Biogeochemical Cycles*, *28*(2), 161–179. https://doi.org/10.1002/2013GB004644

Berry, J., Wolf, A., Campbell, J. E., Baker, I., Blake, N., Blake, D., et al. (2013). A coupled model of the global cycles of carbonyl sulfide and CO_2: A possible new window on the carbon cycle. *Journal of Geophysical Research: Biogeosciences*, *118*(2), 842–852. https://doi.org/10.1002/jgrg.20068

Bloem, E., Haneklaus, S., Kesselmeier, J., & Schnug, E. (2012). Sulfur fertilization and fungal infections affect the exchange of H_2S and COS from agricultural crops. *Journal of Agricultural and Food Chemistry*, *60*(31), 7588–7596. https://doi.org/10.1021/jf301912h

Byrne, B., Strong, K., Colebatch, O., You, Y., Wunch, D., Ars, S., et al. (2020). Monitoring Urban Greenhouse Gases Using Open-Path Fourier Transform Spectroscopy. *Atmosphere-Ocean*, *58*(1), 25–45. https://doi.org/10.1080/07055900.2019.1698407

Campbell, J. E., Berry, J. A., Seibt, U., Smith, S. J., Montzka, S. A., Launois, T., et al. (2017). Large historical growth in global terrestrial gross primary production. *Nature*, *544*, 84–87. https://doi.org/10.1038/nature22030

Campbell, J. E., Carmichael, G. R., Chai, T., Mena-Carrasco, M., Tang, Y., Blake, D. R., et al. (2008). Photosynthetic Control of Atmospheric Carbonyl Sulfide During the Growing Season. *Science*, *322*, 1085–1088. https://doi.org/10.1126/science.1164015

Campbell, J. E., Whelan, M. E., Berry, J. A., Hilton, T. W., Zumkehr, A., Stinecipher, J., et al. (2017). Plant uptake of atmospheric carbonyl sulfide in coast redwood forests. *Journal of Geophysical Research: Biogeosciences*, *122*(12), 3391–3404. https://doi.org/10.1002/2016JG003703

Carmichael, G. R., Peters, L. K., & Saylor, R. D. (1991). The STEM-II regional scale acid deposition and photochemical oxidant model—I. An overview of model development and applications. *Atmospheric Environment. Part A. General Topics*, *25*(10), 2077–2090. https://doi.org/10.1016/0960-1686(91)90085-L

Coates, C. J. (2014). *The BAMS/EDSS/Models-3 I/O API: User manual.* Raleigh, NC. UNC Institute for the Environment, Environmental Modeling Center. Retrieved from http://www.cmascenter.org/ioapi/

Covenant of Mayors. (2009). *Covenant of mayors official text.*

Feng, S., Lauvaux, T., Newman, S., Rao, P., Ahmadov, R., Deng, A., et al. (2016). Los Angeles megacity: A high-resolution land-atmosphere modelling system for urban CO_2 emissions. *Atmospheric Chemistry and Physics*, *16*(14), 9019–9045. https://doi.org/10.5194/acp-16-9019-2016

GPC. (2014). *Global protocol for community-scale greenhouse gas emission inventories.*

Gurney, K. R., Mendoza, D. L., Zhou, Y., Fischer, M. L., Miller, C. C., Geethakumar, S., & de la Rue du Can, S. (2009). High resolution fossil fuel combustion CO_2 emission fluxes for the United States. *Environmental Science & Technology*, *43*(14), 5535–5541. https://doi.org/10.1021/es900806c

Hardiman, B. S., Wang, J. A., Hutyra, L. R., Gately, C. K., Getson, J. M., & Friedl, M. A. (2017). Accounting for urban biogenic fluxes in regional carbon budgets. *Science of the Total Environment*, *592*, 366–372. https://doi.org/10.1016/j.scitotenv.2017.03.028

Heffter, J. L. (1980). Transport layer depth calculations. *Second joint conference on Applications of air pollution meteorology. New Orleans, LA.*

Hilton, T. W., Whelan, M. E., Zumkehr, A., Kulkarni, S., Berry, J. A., Baker, I. T., et al. (2017). Peak growing season gross uptake of carbon in North America is largest in the Midwest USA. *Nature Climate Change*, *7*(6), 450–454. https://doi.org/10.1038/nclimate3272

Hu, X.-M., Nielsen-Gammon, J. W., & Zhang, F. (2010). Evaluation of three planetary boundary layer schemes in the WRF model. *Journal of Applied Meteorology and Climatology*, *49*(9), 1831–1844. https://doi.org/10.1175/2010JAMC2432.1

ICLEI. (2012). *U.S. Community protocol for accounting and reporting of greenhouse gas emissions.*

IEA. (2016). *Cities are in the frontline for cutting carbon emissions.*

Jia, W., & Zhang, X. (2020). The role of the planetary boundary layer parameterization schemes on the meteorological and aerosol pollution simulations: A review. *Atmospheric Research*, *239*, 104890. https://doi.org/10.1016/j.atmosres.2020.104890

Kennedy, C., Steinberger, J., Gasson, B., Hansen, Y., Hillman, T., Havránek, M., et al. (2009). Greenhouse gas emissions from global cities. *Environmental Science and Technology*, *43*(19), 7297–7302. https://doi.org/10.1021/es900213p

Knox, S. H., Windham-Myers, L., Anderson, F., Sturtevant, C., & Bergamaschi, B. (2018). Direct and indirect effects of tides on ecosystem-scale CO_2 exchange in a brackish tidal marsh in northern California. *Journal of Geophysical Research: Biogeosciences*, *123*(3), 787–806. https://doi.org/10.1002/2017JG004048

Kooijmans, L. M. J., Maseyk, K., Seibt, U., Sun, W., Vesala, T., Mammarella, I., et al. (2017). Canopy uptake dominates nighttime carbonyl sulfide fluxes in a boreal forest. *Atmospheric Chemistry and Physics*, *17*(18), 11453–11465. https://doi.org/10.5194/acp-17-11453-2017

Kramer, K., Leinonen, I., Bartelink, H. H., Berbigier, P., Borghetti, M., Bernhofer, C., et al. (2002). Evaluation of six process-based forest growth models using eddy-covariance measurements of CO_2 and H_2O fluxes at six forest sites in Europe. *Global Change Biology*, *8*(3), 213–230. https://doi.org/10.1046/j.1365-2486.2002.00471.x

Krupa, S. V., & Manning, W. J. (1988). Atmospheric ozone: Formation and effects on vegetation. *Environmental Pollution*, *50*(1–2), 101–137. https://doi.org/10.1016/0269-7491(88)90187-X

LaFranchi, B. W., Petron, G., Miller, J. B., Lehman, S. J., Andrews, A. E., Dlugokencky, E. J., et al. (2013). Constraints on emissions of carbon monoxide, methane, and a suite of hydrocarbons in the Colorado Front Range using observations of $^{14}CO_2$. *Atmospheric Chemistry and Physics*, *13*(21), 11101–11120. https://doi.org/10.5194/acp-13-11101-2013

Lee, S.-H., Kim, S.-W., Angevine, W. M., Bianco, L., McKeen, S. A., Senff, C. J., et al. (2011). Evaluation of urban surface parameterizations in the WRF model using measurements during the Texas Air Quality Study 2006 field campaign. *Atmospheric Chemistry and Physics*, *11*(5), 2127–2143. https://doi.org/10.5194/acp-11-2127-2011

Levin, I., Hammer, S., Eichelmann, E., & Vogel, F. (2011). Verification of greenhouse gas emission reductions : The prospect of atmospheric. *Philosophical Transactions of the Royal Society A*, *369*(369), 1906–1924. https://doi.org/10.1098/rsta.2010.0249

Maseyk, K., Berry, J. A., Billesbach, D., Campbell, J. E., Torn, M. S., Zahniser, M., & Seibt, U. (2014). Sources and sinks of carbonyl sulfide in an agricultural field in the Southern Great Plains. *Proceedings of the National Academy of Sciences of the United States of America*, *111*(25), 9064–9069. https://doi.org/10.1073/pnas.1319132111

Mays, K. L., Shepson, P., Stirm, B. H., Karion, A., Sweeney, C., & Gurney, K. (2009). Aircraft-based measurements of the carbon footprint of Indianapolis. *Environmental Science and Technology*, *43*(20), 7816–7823. https://doi.org/10.1021/es901326b

McKain, K., Wofsy, S. C., Nehrkorn, T., Eluszkiewicz, J., Ehleringer, J. R., & Stephens, B. B. (2012). Assessment of ground-based atmospheric observations for verification of greenhouse gas emissions from an urban region. *Proceedings of the National Academy of Sciences of the United States of America*, *109*(22), 8423–8428. https://doi.org/10.1073/pnas.1116645109

Melaas, E. K., Wang, J. A., Miller, D. L., & Friedl, M. A. (2016). Interactions between urban vegetation and surface urban heat islands: A case study in the Boston metropolitan region. *Environmental Research Letters*, *11*(5), 054020. https://doi.org/10.1088/1748-9326/11/5/054020

Miller, J. B., Lehman, S. J., Montzka, S. A., Sweeney, C., Miller, B. R., Karion, A., et al. (2012). Linking emissions of fossil fuel CO_2 and other anthropogenic trace gases using atmospheric $^{14}CO_2$. *Journal of Geophysical Research*, *117*(D8), D08302. https://doi.org/10.1029/2011JD017048

Montzka, S. A., Calvert, P., Hall, B. D., Elkins, J. W., Conway, T. J., Tans, P. P., & Sweeney, C. S. (2007). On the global distribution, seasonality, and budget of atmospheric carbonyl sulfide (COS) and some similarities to CO_2. *Journal of Geophysical Research*, *112*(9), 1–15. https://doi.org/10.1029/2006JD007665

NACP. (2010). *Vulcan CO2 inventory.*

NACP. (2015). *NACP-KAWA-01: CASA GFED3 MERRA flux.*

NASA and USGS. (2017). *MODIS/Terra vegetation Indices.*

Newman, S., Jeong, S., Fischer, M. L., Xu, X., Haman, C. L., Lefer, B., et al. (2013). Diurnal tracking of anthropogenic CO_2 emissions in the Los Angeles basin megacity during spring 2010. *Atmospheric Chemistry and Physics*, *13*(8), 4359–4372. https://doi.org/10.5194/acp-13-4359-2013

NOAA. (2015). Global monitoring laboratory (GML).

NOAA. (2017). Global forecast system (GFS).

NOAA/ESRL. (2015). Radiosonde Database. Retrieved from https://ruc.noaa.gov/raobs/

Park, C., Gerbig, C., Newman, S., Ahmadov, R., Feng, S., Gurney, K. R., et al. (2018). CO_2 transport, variability, and budget over the Southern California Air Basin using the high-resolution WRF-VPRM model during the CalNex 2010 campaign. *Journal of Applied Meteorology and Climatology*, *57*(6), 1337–1352. https://doi.org/10.1175/JAMC-D-17-0358.1

Pataki, D. E., Carreiro, M. M., Cherrier, J., Grulke, N. E., Jennings, V., Pincetl, S., et al. (2011). Coupling biogeochemical cycles in urban environments: Ecosystem services, green solutions, and misconceptions, *Frontiers in Ecology and the Environment*, *9*, 27–36. https://doi.org/10.1890/090220

Pugh, T. A. M., Müller, C., Arneth, A., Haverd, V., & Smith, B. (2016). Key knowledge and data gaps in modelling the influence of CO_2 concentration on the terrestrial carbon sink. *Journal of Plant Physiology*, 3–15. https://doi.org/10.1016/j.jplph.2016.05.001

Rastogi, B., Berkelhammer, M., Wharton, S., Whelan, M. E., Itter, M. S., Leen, J. B., et al. (2018). Large uptake of atmospheric OCS observed at a moist old growth forest: Controls and implications for carbon cycle applications. *Journal of Geophysical Research: Biogeosciences*, *123*(11), 3424–3438. https://doi.org/10.1029/2018JG004430

Riley, W. J. (2005). Influence of terrestrial ecosystems and topography on coastal CO_2 measurements: A case study at Trinidad Head, California. *Journal of Geophysical Research*, *110*(G1), 1–15. https://doi.org/10.1029/2004JG000007

Sandoval-Soto, L., Stanimirov, M., von Hobe, M., Schmitt, V., Valdes, J., Wild, A., & Kesselmeier, J. (2005). Global uptake of carbonyl sulfide (COS) by terrestrial vegetation: Estimates corrected by deposition velocities normalized to the uptake of carbon dioxide (CO_2). *Biogeosciences Discussions*, *2*(1), 183–201. https://doi.org/10.5194/bgd-2-183-2005

Sitch, S., Huntingford, C., Gedney, N., Levy, P. E., Lomas, M., Piao, S. L., et al. (2008). Evaluation of the terrestrial carbon cycle, future plant geography and climate-carbon cycle feedbacks using five dynamic global vegetation models (DGVMs). *Global Change Biology*, *14*(9), 2015–2039. https://doi.org/10.1111/j.1365-2486.2008.01626.x

Skamarock, W. C., Klemp, J. B., Dudhia, J., Gill, D. O., Barker, D. M., Huang, X. Y., et al. (2008). *A Description of the Advanced Research WRF Version 3 (Technical report NCAR/TN–475+STR)*.

Speak, A., Escobedo, F. J., Russo, A., & Zerbe, S. (2020). Total urban tree carbon storage and waste management emissions estimated using a combination of LiDAR, field measurements and an end-of-life wood approach. *Journal of Cleaner Production*, *256*, 120420. https://doi.org/10.1016/j.jclepro.2020.120420

Spielmann, F. M., Wohlfahrt, G., Hammerle, A., Kitz, F., Migliavacca, M., Alberti, G., et al. (2019). Gross primary productivity of four European Ecosystems Constrained by Joint CO_2 and COS Flux Measurements. *Geophysical Research Letters*, *46*(10), 5284–5293. https://doi.org/10.1029/2019GL082006

Stimler, K., Berry, J. A., Montzka, S. A., & Yakir, D. (2011). Association between Carbonyl Sulfide Uptake and ^{18}D during Gas Exchange in C_3 and C_4 Leaves. *Plant Physiology*, *157*(1), 509–517. https://doi.org/10.1104/pp.111.176578

Sweeney, C., Karion, A., Wolter, S., Newberger, T., Guenther, D., Higgs, J. A., et al. (2015). Seasonal climatology of CO_2 across north america from aircraft measurements in the NOAA/ESRL global greenhouse gas reference network. *Journal of Geophysical Research*, *120*(10), 5155–5190. https://doi.org/10.1002/2014JD022591

Turnbull, J., Rayner, P., Miller, J., Naegler, T., Ciais, P., & Cozic, A. (2009). On the use of $^{14}CO_2$ as a tracer for fossil fuel CO_2: Quantifying uncertainties using an atmospheric transport model. *Journal of Geophysical Research*, *114*(D22), D22302. https://doi.org/10.1029/2009JD012308

Turnbull, J. C., Karion, A., Fischer, M. L., Faloona, I., Guilderson, T., Lehman, S. J., et al. (2011). Assessment of fossil fuel carbon dioxide and other anthropogenic trace gas emissions from airborne measurements over Sacramento, California in spring 2009. *Atmospheric Chemistry and Physics*, *11*(2), 705–721. https://doi.org/10.5194/acp-11-705-2011

Turnbull, J. C., Sweeney, C., Karion, A., Newberger, T., Lehman, S. J., Tans, P. P., et al. (2014). Toward quantification and source sector identification of fossil fuel CO_2 emissions from an urban area: Results from the INFLUX experiment. *Journal of Geophysical Research: Atmosphere*, *120*(1), 292–312. https://doi.org/10.1002/2014JD022555

Turner, A. J., Shusterman, A. A., McDonald, B. C., Teige, V., Harley, R. A., & Cohen, R. C. (2016). Network design for quantifying urban CO_2 emissions: Assessing trade-offs between precision and network density. *Atmospheric Chemistry and Physics*, *16*(21), 13465–13475. https://doi.org/10.5194/acp-16-13465-2016

UN/DESA. (2018). The world's cities in 2018. World urbanization prospects: The 2018 revision. Retrieved from: https://www.un.org/en/events/citiesday/assets/pdf/the_worlds_cities_in_2018_data_booklet.pdf

United Nations/Framework convention on climate change. (2015). *United Nations/Framework Convention on Climate Change. Adoption of the Paris Agreement, 21st Conference of the Parties, Paris: United Nations*.

Velasco, E., Roth, M., Norford, L., & Molina, L. T. (2016). Does urban vegetation enhance carbon sequestration? *Landscape and Urban Planning*, *148*, 99–107. https://doi.org/10.1016/j.landurbplan.2015.12.003

Wei, C., Wang, M., Fu, Q., Dai, C., Huang, R., & Bao, Q. (2020). Temporal characteristics of greenhouse gases (CO_2 and CH_4) in the megacity Shanghai, China: Association with air pollutants and meteorological conditions. *Atmospheric Research*, *235*, 104759. https://doi.org/10.1016/j.atmosres.2019.104759

Whelan, M. E., Min, D. H., & Rhew, R. C. (2013). Salt marsh vegetation as a carbonyl sulfide (COS) source to the atmosphere. *Atmospheric Environment*, *73*, 131–137. https://doi.org/10.1016/j.atmosenv.2013.02.048

Yang, F., Qubaja, R., Tatarinov, F., Rotenberg, E., & Yakir, D. (2018). Assessing canopy performance using carbonyl sulfide measurements. *Global Change Biology*, *24*(8), 3486–3498. https://doi.org/10.1111/gcb.14145

Yi, Z., Wang, X., Sheng, G., & Fu, J. (2008). Exchange of carbonyl sulfide (OCS) and dimethyl sulfide (DMS) between rice paddy fields and the atmosphere in subtropical China. *Agriculture, Ecosystems and Environment*, *123*(1–3), 116–124. https://doi.org/10.1016/j.agee.2007.05.011

Yver, C. E., Graven, H. D., Lucas, D. D., Cameron-Smith, P. J., Keeling, R. F., & Weiss, R. F. (2013). Evaluating transport in the WRF model along the California coast. *Atmospheric Chemistry and Physics*, *13*(4), 1837–1852. https://doi.org/10.5194/acp-13-1837-2013

Zhao, S., Liu, S., & Zhou, D. (2016). Prevalent vegetation growth enhancement in urban environment. *Proceedings of the National Academy of Sciences of the United States of America*, *113*(22), 6313–6318. https://doi.org/10.1073/pnas.1602312113

Zumkehr, A., Hilton, T. W., Whelan, M., Smith, S., Kuai, L., Worden, J., & Campbell, J. E. (2018). Global gridded anthropogenic emissions inventory of carbonyl sulfide. *Atmospheric Environment*, *183*, 11–19. https://doi.org/10.1016/j.atmosenv.2018.03.063